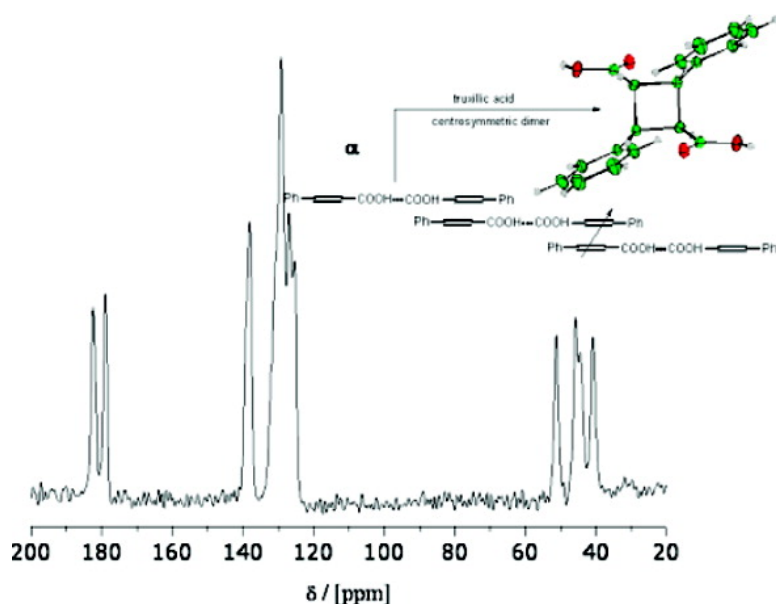


## Transient States in [2 + 2] Photodimerization of Cinnamic Acid: Correlation of Solid-State NMR and X-ray Analysis

Mujeeb Khan, Gunther Brunklaus, Volker Enkelmann, and Hans-Wolfgang Spiess

*J. Am. Chem. Soc.*, **2008**, 130 (5), 1741-1748 • DOI: 10.1021/ja0773711

Downloaded from <http://pubs.acs.org> on February 8, 2009



### More About This Article

Additional resources and features associated with this article are available within the HTML version:

- Supporting Information
- Links to the 5 articles that cite this article, as of the time of this article download
- Access to high resolution figures
- Links to articles and content related to this article
- Copyright permission to reproduce figures and/or text from this article

[View the Full Text HTML](#)

## Transient States in [2 + 2] Photodimerization of Cinnamic Acid: Correlation of Solid-State NMR and X-ray Analysis

Mujeeb Khan, Gunther Brunklaus,\* Volker Enkelmann, and Hans-Wolfgang Spiess

Max-Planck-Institut für Polymerforschung, Postfach 31 48, D-55021 Mainz, Germany

Received September 24, 2007; E-mail: brunklaus@mpip-mainz.mpg.de

**Abstract:**  $^{13}\text{C}$ -CPMAS and other solid-state NMR methods have been applied to monitor the solid-state reactions of *trans*-cinnamic acid derivatives, which are the pioneer and model compounds in the field of topochemistry previously studied by X-ray diffraction, AFM, and vibrational spectroscopy. Single-crystal X-ray analyses of photoirradiated  $\alpha$ -*trans*-cinnamic acid where the monomers are arranged in a head-to-tail manner have revealed the formation of a centrosymmetric  $\alpha$ -truxillic acid photodimer. For a centrosymmetric dimer, however, two cyclobutane carbon signals and one carbonyl carbon signal were expected apart from other aromatic carbon signals. Instead, four cyclobutane and two carbonyl carbon signals were observed suggesting the formation of a *non*-centrosymmetric photodimer. Removing hydrogen bonds from the system by esterification of  $\alpha$ -truxillic acid yield a centrosymmetric photodimer. Careful analysis of the obtained products via solid-state NMR clearly showed that the observed peak splittings in the  $^{13}\text{C}$ -CPMAS spectra did *not* originate from packing effects but rather result from *asymmetric* hydrogen bonds distorting the local symmetry. Further evidence of this rather dynamic hydrogen-bonding stems from high-temperature X-ray data revealing that only the joint approach of both X-ray analysis and solid-state NMR at similar temperatures allows for the successful characterization of dynamic processes occurring in topochemical reactions, thus, providing detailed insight into the reaction mechanism of organic solid-state transformations.

### 1. Introduction

[2 + 2] Photodimerizations are among the most extensively studied organic solid-state reactions.<sup>1–2</sup> A first systematic study concerning the relationship between the chemical reactivity of an organic solid and its crystal structure has been reported by Schmidt and co-workers<sup>3</sup> on the photodimerization of cinnamic acid and its derivatives. The range of reactions that have since then been reported to be topochemically controlled has increased significantly but naturally cannot compete with synthetic chemistry in solution. What has given particular impetus to the study of organic solid-state reactions is the appreciation that the “frozen” state of the reactant can allow a very detailed exploration of the mechanistic aspect of the solid-state reactions.<sup>4</sup> Other developments in the areas of morphology control, crystal growth inhibition, crystal-to-crystal conversions,<sup>5</sup> absolute asymmetric synthesis, and, more recently, supramolecular design<sup>6</sup> and molecular recognition have all impinged on the development of organic solid-state chemistry.

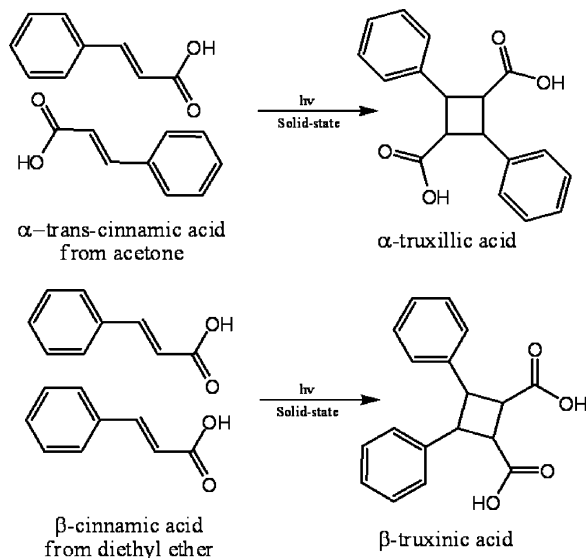
The [2 + 2] photodimerization of *trans*-cinnamic acid (and many of its derivatives<sup>7</sup>) constitutes the classic example of a solid-state reaction that conforms to the topochemical principle.

Numerous studies have been pursued on this class of compounds for basic design, planning, and understanding of the solid-state reactions.<sup>8</sup> Schmidt et al.<sup>3</sup> have classified the packing of *trans*-cinnamic acid and its derivatives in three different forms: an  $\alpha$ -form (where monomers are arranged in a head-to-tail manner),  $\beta$ -form (with the monomers arranged head-to-head), and a  $\gamma$ -form (where the monomers are unfavorably aligned). While in both the  $\alpha$ - and  $\beta$ -forms the reactive double bonds approach each other by less than approximately 4 Å and which are photoactive yielding head-to-tail and head-to-head dimers, respectively (Scheme 1), the  $\gamma$ -form is photostable. The topotactic nature of the obtained reaction products has been revealed by applying various techniques such as atomic force microscopy (AFM),<sup>9</sup> vibrational spectroscopy,<sup>10</sup> X-ray diffraction,<sup>11,12</sup> and solid-state NMR.<sup>13–16</sup> Since AFM is primarily sensitive to

- (1) Tanaka, K.; Toda, F. *Chem. Rev.* **2000**, *100*, 1025–1074.
- (2) Ramamurthy, V.; Venkatesan, K. *Chem. Rev.* **1987**, *87*, 433–481.
- (3) Schmidt, G. M. J. *Pure Appl. Chem.* **1971**, *27*, 647–678.
- (4) McBride, J. M.; Segmüller, B. E.; Hollingsworth, M.; Mills, D. E.; Weber, B. A. *Science* **1986**, *234*, 830–835.
- (5) Tomislav, F.; MacGillivray, L. R. Z. *Kristallogr.* **2005**, *220*, 351–363.
- (6) Desiraju, G. J. *Angew. Chem., Int. Ed. Engl.* **1995**, *34*, 2311–2327.
- (7) Schmidt, G. M. J. *J. Chem. Soc.* **1964**, 2014–2021.

- (8) Ghosh, M.; Chakrabarti, S.; Misra, T. N. *J. Raman Spectrosc.* **1998**, *29*, 263–267. (b) Atkinson, S. D. M.; Almond, M. J.; Bowmaker, G. A.; Drew, M. G. B.; Feltham, E. J.; Hollins, P.; Jenkins, S. L.; Wiltshire, K. S. *J. Chem. Soc., Perkin Trans. 2* **2002**, *9*, 1533–1537. (c) Davaasambuu, J.; Busse, G.; Techert, S. *J. Phys. Chem. A* **2006**, *110*, 3261–3265. (d) Jenkins, S. L.; Almond, M. J.; Atkinson, S. D. M.; Drew, M. G. B.; Hollins, P.; Mortimore, J. L.; Tobin, M. J. *J. Mol. Struct.* **2006**, *786*, 220–226.
- (9) Kaupp, G. *Angew. Chem., Int. Ed. Engl.* **1992**, *31*, 592–595. (b) Kaupp, G. *Angew. Chem.* **1992**, *104*, 606–609.
- (10) Samantha, D. M.; Matthew, J. A.; Bruneel, J.; Amdrew, G.; Hollins, P.; Mascetti, J. *Spectrochim. Acta* **2000**, *A56*, 2423–2430.
- (11) Enkelmann, V.; Wegner, G.; Novak, K. *J. Am. Chem. Soc.* **1993**, *115*, 10390–10391.
- (12) Abdelmoty, I.; Buchholz, V.; Di, L.; Enkelmann, V.; Wegner, G.; Foxman, B. M. *Cryst. Growth Des.* **2005**, *17*, 2210–2217.
- (13) Stitchell, S. G.; Harris, K. D. M.; Aliev, A. E. *Struct. Chem.* **1994**, *5*, 327–333.
- (14) Hilgeroth, A.; Hempel, G.; Baumeister, U.; Reichert, D. *Solid State Nucl. Magn. Reson.* **1999**, *13*, 231–243.

**Scheme 1.** Diagram Illustrating the Conversion of the  $\alpha$ - and  $\beta$ -Forms of *trans*-Cinnamic Acid to Dimers via Topotactic Reactions



surfaces, structural information cannot be obtained directly. In contrast, vibrational spectroscopy monitors the topotactic nature of organic solid-state reactions, but conformational details of possible intermediate states remain vague.

X-ray crystallography is an excellent tool to investigate photodimerization reactions of single crystals. However, many crystals tend to shatter into microcrystalline particles as the dimerization proceeds, rendering an X-ray analysis of obtained products difficult. Previously, we reported the topochemically controlled single-crystal-to-single-crystal transformation of  $\alpha$ -*trans*-cinnamic acid into  $\alpha$ -truxillic acid.<sup>11</sup> Utilizing a selective reaction procedure where the photoactive crystals are irradiated by light for which they have low absorptivity, even crystals (and their corresponding X-ray structures) at intermediate stages of the photodimerization were obtained. These can be characterized as substitutional mixed crystals in which the dimer and monomer pair occupies the same lattice site with an occupancy according to the conversion. A severe limitation of this technique stems from the fact that it is not suitable for the characterization of either amorphous or rather ill-defined solids that lack long-range translational order. In addition, the localization of lighter atoms (e.g., hydrogen-bonded protons)<sup>17</sup> may be difficult even with sophisticated X-ray diffraction methods.<sup>18</sup>

Recently, it has been demonstrated that solid-state NMR can also be successfully applied to monitor organic solid-state photoreactions.<sup>13–16</sup> Its unique selectivity allows for the differentiation of chemically distinct sites, including protons,<sup>19</sup> on the basis of the NMR chemical shift.<sup>20</sup> Thus, solid-state NMR reveals molecular species present in the sample, including products, reactants, and possible side products as well as polymorphs.<sup>21</sup> Hence, the combination of solid-state NMR and (single crystal) X-ray analysis to study topochemical reactions

provides in-depth information about the topotactic nature of the reactions as well as structural changes that occurred at the molecular level during the reaction.

In this paper, we return to certain “missing links” in the evolving story of crystalline state [2 + 2] cycloadditions. We have applied single-crystal X-ray analysis as well as solid-state NMR to monitor the [2 + 2] photodimerization of  $\alpha$ -*trans*-cinnamic acid to  $\alpha$ -truxillic acid. Crystal structures<sup>11,12</sup> suggest that  $\alpha$ -truxillic acid is a centrosymmetric photodimer. During the course of our study, however, <sup>13</sup>C-CPMAS spectra were reported for different conversion ratios ranging from  $\alpha$ -*trans*-cinnamic acid (0%) to  $\alpha$ -truxillic acid (100%).<sup>15</sup> In contrast to an anticipated centrosymmetric molecular geometry of  $\alpha$ -truxillic acid, the <sup>13</sup>C-CPMAS spectra exhibited additional signals for the cyclobutane ring and carbonyl region, which Hayes et al.<sup>15</sup> attributed to solid-state packing effects, e.g., distortions in the cyclobutane ring and/or dihedral angle twists of both the phenyl rings and carboxylic acid group. Alternatively, however, the observed signal splittings may originate from (possibly asymmetric) hydrogen bondings, which not only are known to distinctly impact <sup>13</sup>C or <sup>15</sup>N spectra<sup>22,23</sup> but also more importantly are revealed by characteristic chemical shifts of up to 21 ppm in the respective solid-state proton NMR spectra.<sup>23,24</sup> Indeed, the comparison of both X-ray and NMR data turned out to be very fruitful in many different cases,<sup>23,25</sup> but proper care of the temperature settings must be taken.

In order to clearly distinguish the two possible sources of peak splitting, we have synthesized not only mixed crystals of photodimers at various conversion ratios but also the methyl ester of truxillic acid. Moreover, as the hydrogen bonding can be of dynamic nature, the X-ray structures of photodimerized  $\alpha$ -*trans*-cinnamic acid obtained at low (e.g., liquid helium-cooled) and high temperatures (350 K) are compared and discussed with respect to the recorded <sup>13</sup>C-CPMAS NMR spectra.

## 2. Experimental Section

*trans*-Cinnamic acid (Aldrich, 99%) was recrystallized from acetone (Aldrich) to obtain the  $\alpha$ -polymorph. The crystals were ground to small microcrystalline particles, and about 400 mg of product were evenly distributed in a thin layer on a 100 mm Petri dish and placed in the focus of the lamp for irradiation. The powder sample was exposed to broad band irradiation (material exposed to both tail irradiation<sup>11</sup> and broad band irradiation produced the same structure, except that samples obtained by tail irradiation resulted in intact crystals suitable for single-crystal X-ray analysis) using a 100 W high-pressure Hg lamp (Muller electronic LXH100) for a period of 10 h to obtain 100% converted

- (15) Bertmer, M.; Nieuwendaal, R. C.; Barnes, A. B.; Hayes, S. E. *J. Phys. Chem. B* **2006**, *110*, 6270–6273.  
 (16) Harris, K. D. M.; Thomas, J. M. *J. Solid State Chem.* **1991**, *94*, 197–205.  
 (17) Brown, S. P.; Spiess, H. W. *Chem. Rev.* **2001**, *101*, 4125–4155. (b) Harris, R. K. *Solid State Sci.* **2004**, *6*, 1025–1037.  
 (18) Harris, K. D. M.; Cheung, E. Y. *Chem. Soc. Rev.* **2004**, *33*, 526–538.  
 (19) Brown, S. P. *Prog. Nucl. Magn. Reson. Spectrosc.* **2007**, *50*, 199–251.  
 (20) Harris, R. K. *Solid State Sci.* **2004**, *6*, 1025–1037.  
 (21) Harris, R. K. *The Analyst* **2006**, *131*, 351–373.

- (22) Schilf, W.; Kamiński, B.; Szady-Chelmienicka, A.; Grech E. *J. Mol. Struct.* **2004**, *700*, 105–108.  
 (23) Gobetto, R.; Nervi, C.; Chierotti, M. R.; Braga, D.; Maini, L.; Harris, K. R.; Hodgkinson, P. *Chem.–Eur. J.* **2005**, *11*, 7461–7471.  
 (24) (a) Li, S.; Zheng, S.; Su, Y.; Zhang, H.; Chen, L.; Yang, J.; Ye, C.; Deng, F. *J. Am. Chem. Soc.* **2007**, *129*, 11161–11171. (b) Yates, J. R.; Pham, T. N.; Pickard, C. J.; Mauri, F.; Amando, A. M.; Gil, A. M.; Brown, S. P. *J. Am. Chem. Soc.* **2005**, *127*, 10216–10220. (c) Riedel, K.; Leppert, J.; Ohlenschlaeger, O.; Goerlach, M.; Ramachandran, R. *J. Biomol. NMR* **2005**, *31*, 331–336. (d) Brus, J.; Dybal, J. *Macromol.* **2002**, *35*, 10038–10047. (e) Brown, S. P.; Zhu, X. X.; Saalwaechter, K.; Spiess, H. W. *J. Am. Chem. Soc.* **2001**, *123*, 4275–4285. (f) Schnell, I.; Brown, S. P.; Low, H. Y.; Ishida, H.; Spiess, H. W. *J. Am. Chem. Soc.* **1998**, *120*, 11784–11795.  
 (25) (a) Fyfe, C. A.; Brouwer, D. H.; Lewis, A. R.; Villaescusa, L. A.; Morris, R. E. *J. Am. Chem. Soc.* **2002**, *124*, 7770–7778. (b) Liu, H.; Roger, M.; Hanson, J. C.; Grey, C. P.; Martin, J. D. *J. Am. Chem. Soc.* **2001**, *123*, 7564–7573. (c) Grey, C. P.; Poshni, F. I.; Gualtieri, A. F.; Norby, P.; Hanson, J. C.; Corbin, D. R. *J. Am. Chem. Soc.* **1997**, *119*, 1981–1989. (d) Schaller, T.; Buechele, U. P.; Klaerner, F. G.; Blaeser, D.; Boese, R.; Brown, S. P.; Spiess, H. W. *J. Am. Chem. Soc.* **2007**, *129*, 1293–1303.

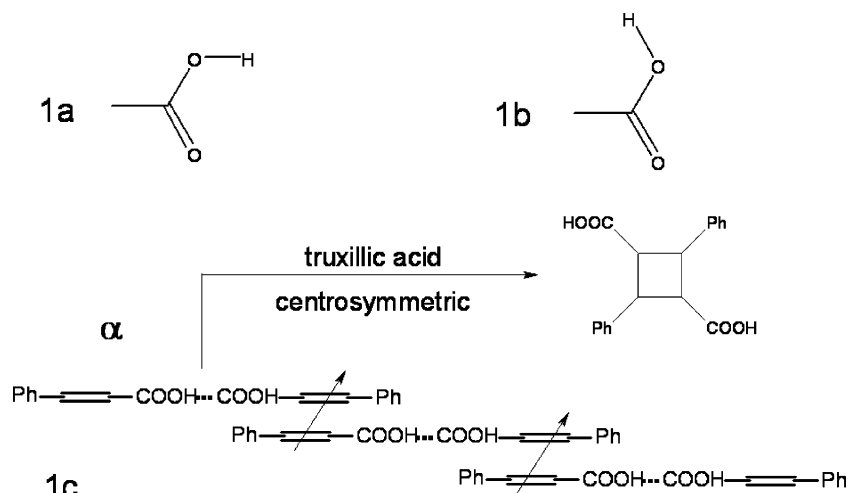


**Figure 1.** O–H group conformation in carboxylic acids and packing mode of  $\alpha$ -*trans*-cinnamic acid in crystal lattice. (a) Synplanar conformation of carboxyl group. (b) Antiplanar conformation. (c) Schematic view of the  $\alpha$ -modification of cinnamic acid.

as-dimerized truxillic acid ( $P2_1/n$  phase<sup>12</sup>), which was confirmed by powder diffraction data provided in the Supporting Information. (Powder diffraction data are also given for the Donnay polymorph of truxillic acid ( $C2/c$  phase<sup>12</sup>) that was obtained by recrystallization of small amounts of 100% converted as-dimerized truxillic acid from acetone.) About 100 mg of product were taken out at each interval of 2 h for solid-state NMR measurements. In order to obtain fast conversion, the powder was agitated after every 30 min and was simultaneously rotated using a home-built small rotating machine. Single crystals of  $\alpha$ -*trans*-cinnamic acid were obtained by slow evaporation of an acetone solution; crystals were then irradiated by a tail irradiation technique using a 345 nm edge filter to obtain intact crystals of  $P2_1/n$  phase truxillic acid. A suitable single crystal was picked up from the sample, and crystal structures were determined on that crystal at different temperatures to investigate the temperature dependency of the bond length. The deuterated samples of *trans*-cinnamic acid and truxillic acid were obtained by using ethanol- $d_6$  (Carl Roth). About 100 mg of product were dissolved in 5 mL of solvent and left for slow evaporation.

**Synthesis of Methyl Ester of Truxillic Acid:** Methyl ester of truxillic acid (dimethyl 2, 4-diphenylcyclobutane-1, 3-dicarboxylate) was synthesized by a simple esterification reaction. Truxillic acid (250 mg, 0.84 mmol) was dissolved in 30 mL of methanol in a 50 mL round bottomed flask; to this solution about 0.5 mL of thionyl chloride ( $\text{SOCl}_2$ ) was added, and the mixture was allowed to reflux until TLC analysis indicated a complete reaction. The mixture was then concentrated in vacuo, and the residue was taken up in 50 mL of methylene chloride and washed with  $3 \times 50$  mL of water. The organic layer was dried over  $\text{Na}_2\text{SO}_4$ . Removal of the solvent in vacuo afforded a white powder which was then purified over a short silica gel column using acetone and petrol ether as eluent in a 1:9 ratio. Evaporation of the solvent afforded 248 mg of a white crystalline solid (methyl ester of truxillic acid) in 90% yield. Single crystals of methyl truxillic acid for X-ray analysis were obtained by the slow evaporation of an acetone solution.  $^1\text{H}$  NMR,  $\delta$ : 7.38–7.26 (M, 10H, Ar); 4.47 (T, 2H, Ar–CH–CH); 4.02 (T, 2H, OOC–CH–CH); 3.30 (S, 6H, O–CH<sub>3</sub>). EI MS:  $m/z$  324 ( $\text{M}^+$ ). Mp = 175 °C.

**Solid-State NMR:** All  $^{13}\text{C}$ -CPMAS spectra were collected at 125.77 MHz (Bruker Avance 500 spectrometer), with a CP-contact time of 5 ms coadding 4096 transients. The experiments were carried out using a standard Bruker 2.5 mm double resonance MAS probe spinning at 25 kHz, with a typical  $\pi/2$ -pulse length of 2.5  $\mu\text{s}$  and a recycle delay of 15 s. The spectra are referenced with respect to tetramethyl silane (TMS) using adamantane as a secondary standard (29.46 ppm for  $^{13}\text{C}$ ).<sup>26</sup> If not stated otherwise, all spectra were acquired at room temperature.

Static, variable-temperature  $^2\text{H}$  quadrupolar echo spectra<sup>27</sup> were recorded at 46.07 MHz using a home-built 7 mm probe and a Bruker Avance-II 300 spectrometer. The interpulse delay was set to 20  $\mu\text{s}$ , and the  $\pi/2$ -pulse length, to 2  $\mu\text{s}$ . The temperature was varied from 240 to 400 K. Typically, 8096 scans were accumulated.

**Solution NMR and Mass:** The solution NMR spectra were recorded on a Bruker AC 250. The residual  $^1\text{H}$  peak of the deuterated solvent was used as an internal standard (Acetone,  $^1\text{H}$ ,  $\delta = 2.05$  ppm). The mass spectrum was obtained using a Varian Mat 7a (70e.v.).

**DFT-Based Chemical Shift Calculations:** Geometry optimizations were performed based on the available crystal structures using the BLYP functional<sup>28</sup> and 6-311G<sup>29</sup> split valence basis set augmented with diffuse and polarization functions. Subsequently,  $^{13}\text{C}$  chemical shifts with respect to tetramethyl silane (TMS) were computed at the B3LYP/6-311++G (2df, 2pd) level of theory with the GIAO approach as implemented in the Gaussian98 program package.<sup>30</sup>

**Single-Crystal X-ray Analysis:** All X-ray structures were recorded on a Kccd diffractometer with graphite monochromated Mo K $\alpha$  radiation. Lattice parameters were obtained by least-squares fits to the scattering angles of reflections observed in several prescans. The intensity data collection was performed by  $\phi$  and  $\omega$  scans. The raw data were corrected for Lorentz and polarization effects. The structures were solved by direct methods and refined by full matrix least-squares analyses with anisotropic temperature factors for all atoms except H. Positions of the H atoms were calculated using the known molecular geometry and refined in the riding mode with fixed isotropic temperature factors. Empirical absorption corrections were applied to the data.

### 3. Results and Discussion

The carboxyl group in the majority of mono- and dicarboxylic acids in its crystalline phase adopt either a synplanar (1a) or antiplanar (1b) O=C–O–H conformation as shown in Figure 1.<sup>31,32</sup> The synplanar structure is the more stable conformer while the antiplanar form usually occurs when the O–H bond participates in an intramolecular O–H $\cdots$ O bond.  $\alpha$ -*trans*-Cinnamic acid, a nonsubstituted acid, which does not involve

(26) Morkombe, C. R.; Zilm, K. *J. Magn. Reson.* **2003**, *162*, 479–486.

(27) Furo, I.; Hedin, N. *J. Magn. Reson.* **2001**, *152*, 214–216.

(28) (a) Becke, A. D. *Phys. Rev.* **1988**, *A38*, 3098–3100. (b) Lee, C.; Yang, W.; Parr, R. G. *Phys. Rev.* **1988**, *A37*, 785–789.

(29) Krishnan, R.; Binkley, J. S.; Seger, R.; Pople, J. A. *J. Chem. Phys.* **1980**, *72*, 650–654.

(30) Frisch, M. J., et al. *Gaussian 98*, revision A.7; Gaussian Inc.: Pittsburgh, PA, 1998.

(31) Leiserowitz, L. *Acta Crystallogr.* **1976**, *B32*, 775–802.

(32) Miyazawa, T.; Pitzer, K. S. *J. Am. Chem. Soc.* **1959**, *81* (1), 74–79.

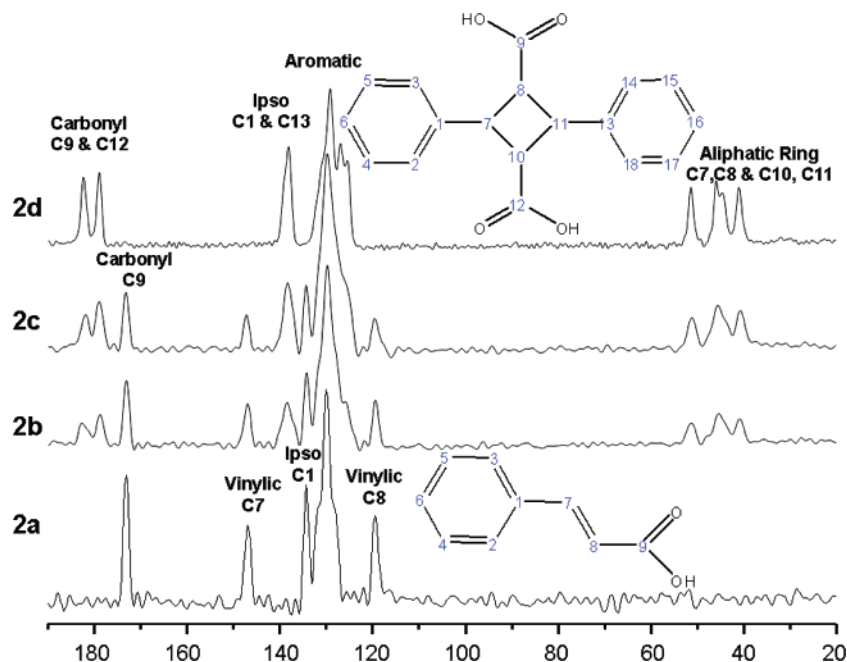


**Figure 2.** Solid-state  $^{13}\text{C}$ -CPMAS spectra ranging from  $\alpha$ -*trans*-cinnamic acid to  $\alpha$ -truxillic acid: (a) monomer prior to irradiation, (b)  $\sim 25\%$  converted mixture, (c)  $\sim 50\%$  converted mixture, (d) dimer after complete conversion (as-dimerized,  $P2_1/n$  phase).  $^{13}\text{C}$ -CPMAS spectrum of another polymorph of truxillic acid, i.e., recrystallized truxillic acid  $C2/c$  phase,<sup>12</sup> was also measured and is provided in the Supporting Information. Surprisingly there is not a very distinct difference between the  $^{13}\text{C}$ -CPMAS spectra of  $P2_1/n$  and  $C2/c$  phases which can be easily distinguished by their powder patterns provided also in the Supporting Information.

in any kind of intramolecular hydrogen bonding adopts a synplanar conformation with respect to its carboxyl group. However, units of two monomers which are approximately in the same plane and connected via *intermolecular* hydrogen bonds form highly overlapped parallel stacks getting monomers within certain distances and relative orientations into close contact. In the  $\alpha$ -form, the overlap offset is so large that the closest monomer pairings in a reactive orientation are not in the same stack but in neighboring stacks. Thus, while neighbors within the same stack are related by mirror symmetry and are over  $5.5 \text{ \AA}$  apart, the reacting pairs are only  $4 \text{ \AA}$  apart. Therefore, in an  $\alpha$ -lattice head-to-tail centrosymmetric dimers are formed with the least lattice disturbance.<sup>11–12,33</sup>

A series of  $^{13}\text{C}$ -CPMAS NMR spectra for  $\alpha$ -*trans*-cinnamic acid and the corresponding  $[2 + 2]$  photodimerization products after various irradiation times were reported by Hayes et al.<sup>15</sup> They showed that solid-state NMR can be successfully applied to study this class of photodimerization reactions because of the good resolution of individual resonances and the large separation of the signals of reactant and product functional groups. In contrast to an anticipated centrosymmetric molecular geometry of  $\alpha$ -truxillic acid, the  $^{13}\text{C}$ -CPMAS spectra exhibited additional signals for the cyclobutane ring and carbonyl region, which Hayes et al.<sup>15</sup> referred to as solid-state packing effects, e.g., distortions in the cyclobutane ring and/or dihedral angle twists of both the phenyl rings and carboxylic acid group. Careful observation of the crystal structures of mixtures as well as fully converted truxillic acid did not reveal *any* distortions or packing defects in the crystal lattice.

Even computed  $^{13}\text{C}$  chemical shifts of the  $\alpha$ -truxillic acid dimer based on an optimized X-ray geometry revealed *neither* any splitting in the carbonyl region *nor* any extra signals in the

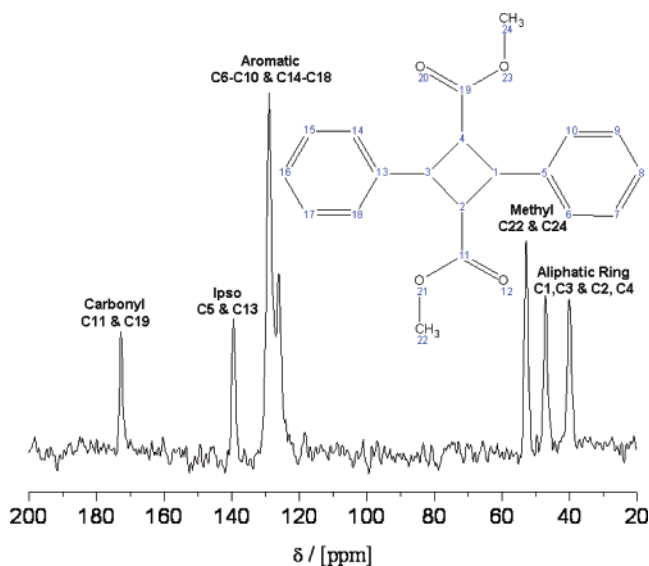
cyclobutane ring region. This prompted us to consider the consequences of (possibly dynamic) hydrogen bonding present in the crystals. Indeed, each  $\alpha$ -truxillic acid photodimer is hydrogen bonded to *two* of its neighboring molecules forming a chainlike structure.<sup>12</sup> Since X-ray methods suffer from the fact that heavy atoms tend to dominate the observed diffraction pattern, it is difficult to locate lighter atoms (e.g., hydrogen) accurately. In this case, solid-state NMR can provide complementary information. Figure 2 shows a series of  $^{13}\text{C}$ -CPMAS NMR spectra ranging from  $\alpha$ -*trans*-cinnamic (0% conversion) to as-dimerized  $\alpha$ -truxillic acid ( $P2_1/n$  phase,<sup>12</sup> 100% conversion), where Figure 2b and 2c are spectra for partial mixtures containing both monomer and dimer at  $\sim 25\%$  and  $\sim 50\%$  conversion, respectively.

As the dimerization proceeds, the corresponding intensities of both the olefinic carbon and carbonyl carbon signals assigned to the monomer decreased with a gradual rise of the new carbon signals attributed to the cyclobutane ring indicating the successful formation of a photodimer. Additionally, the chemical shifts of the neighboring carbons, i.e., the *ipso* (non protonated) carbon and the carbonyl carbon, display a small downfield shift upon conversion of the monomer into a dimer, possibly due to differences in inductive effects of neighboring groups (vinyl vs cyclobutane). The complete assignments of the carbon sites in all samples are given in Table 1. Two signals in the carbonyl region and four different signals in the cyclobutane ring are observed in both partially and fully converted dimer spectra (Figure 2b–d). In contrast, the solution  $^{13}\text{C}$  NMR spectrum exhibits only two peaks in the cyclobutane ring and a single peak in the carbonyl region (as expected from centrosymmetric molecular geometry). The latter resonance is downfield shifted from 173 ppm in solution to about 179 ppm in the solid state, probably due to hydrogen bondings that are absent in solution.

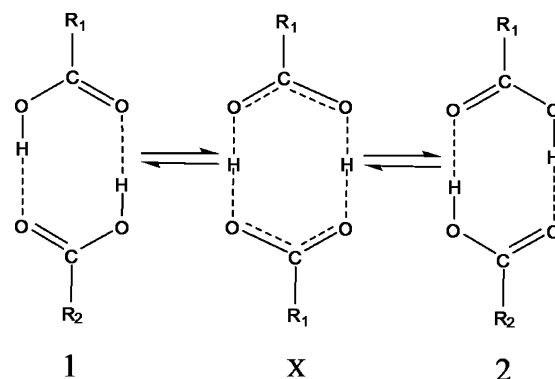
(33) Cohen, M. C.; Schmidt, G. M. J.; Sonntag, F. I. *J. Chem. Soc.* **1964**, 2000–2013.

**Table 1.** Resonance Assignments for  $\alpha$ -*trans*-Cinnamic Acid,  $\alpha$ -Truxillic Acid, and  $\alpha$ -Truxillic Acid Methyl Ester Based on *ab Initio* Chemical Shift Calculations

sample	$\delta$ (ppm)	assignment
$\alpha$ - <i>trans</i> -cinnamic acid	173.1	carbonyl carbon (C9)
	146.9	vinyl carbon (C7)
	134.3	ipso carbon (C1)
	131.2–127.8	aromatic carbons (C2–C6)
$\alpha$ -truxillic acid	119.4	vinyl carbon (C8)
	182.3	carbonyl carbon (COO <sup>-</sup> )
	178.9	carbonyl carbon (COOH)
	138.0	ipso carbons (C1, C13)
	129.6	aromatic (C2, C3, C14, and C18)
	126.6	aromatic (C4, C5, C15, and C17)
	125.5	aromatic (C6, C16)
	52.1	cyclobutane ring carbon (C8)
	46.2	cyclobutane ring carbon (C10)
	45.1	cyclobutane ring carbon (C7)
	41.3	cyclobutane ring carbon (C11)
$\alpha$ -truxillic acid methyl ester	172.7	carbonyl carbon (C11, C19)
	139.4	ipso carbon (C5, C13)
	126.1–128.9	aromatic carbons
	52.8	methyl carbons (C22, C24)
	47.1	aliphatic carbons (C2, C4)
	40.0	aliphatic carbons (C1, C3)

**Figure 3.** Solid-state  $^{13}\text{C}$ -CPMAS of truxillic acid methyl ester (dimethyl-2,4-diphenylcyclobutane-1,3-dicarboxylate).

To further explore possible influences of hydrogen bonding in the solid compounds, we prepared the methyl ester of  $\alpha$ -truxillic acid. The corresponding  $^{13}\text{C}$ -CPMAS spectrum (cf. Figure 3) unambiguously reflects a centrosymmetric photodimer; that is, there are three signals in the aliphatic region: one is assigned to methyl carbon and the other two signals belong to the cyclobutane ring. Symmetry renders the two carbons attached to the carbonyl groups or phenyl rings equivalent. Moreover, the  $^{13}\text{C}$  chemical shifts of the ester compound are close to those  $^{13}\text{C}$  shift values obtained for  $\alpha$ -truxillic acid in solution (i.e.,  $\sim 173$  ppm for carbonyl carbon). Taken together, this strongly suggests that any observed excess signals are not due to solid-state packing effects but rather due to asymmetry of the (dynamic) hydrogen bonds which temporarily destroys the center of symmetry of the  $\alpha$ -truxillic acid photodimer.

**Figure 4.** Interconversion of the molecular structure of a carboxylic acid dimer.<sup>34</sup>**Dynamics of Hydrogen Bonds in Carboxylic Acid Dimers:**

After concluding that the distortion of the symmetry is mainly caused by hydrogen bonds, we were concerned with the possible dynamics of the hydrogen-bonded pair. In the past, numerous studies have been published about the dynamics of hydrogen atoms in carboxylic acid dimers suggesting various models to describe the motion of the hydrogen along the hydrogen bond.<sup>34–38</sup> The best suited approach in the case of  $\alpha$ -truxillic acid is given by Horsewill and Aibout.<sup>38</sup> It states that (di-)carboxylic acids not only commonly yield centrosymmetric dimers in the solid state where a ringlike structure is formed by *two* hydrogen bonds (cf. Figure 4) but also arrange as continuous polymeric chains of molecules stabilized by hydrogen bonds. This also exists in truxillic acid crystals.<sup>12</sup> Within a single dimer unit two conformations, labeled 1 and 2, are possible. The interconversion between the two configurations 1 and 2 should involve a simultaneous proton exchange across a symmetric transition structure X. Due to this effect the potential energy of the system with respect to the hydrogen atom position can conveniently be described with a double minimum, while in the solid state the influence of neighboring molecules breaks the symmetry of the potential so that the two potential wells may in general be of unequal depth. It is possible for the hydrogen atoms to move in a coordinated fashion within the ring established by the two hydrogen bonds resulting in a change of the electronic structure and atomic arrangement within the dimer; e.g., a C=O bond turns into a C–O bond and *vice versa*.

In the case of  $\alpha$ -truxillic acid, proton dynamics studies<sup>34–38</sup> suggest that either a thermally activated proton transfer takes place or tunneling occurs. This could be addressed in detail by either  $T_1$  relaxation measurements or (quasi)inelastic neutron scattering.

**Structural Correlations from Solid State and Crystal Structure Analysis:** Considering the double minimum potential approach, one might expect *two* different acidic proton peaks in the  $^1\text{H}$  MAS NMR spectrum of the truxillic acid, but the corresponding spectrum (cf. Figure 5) displays only two signals: a broad signal with a small shoulder represents both the aliphatic and aromatic protons, while the single peak at  $\sim 14$  ppm (fwhh = 1000 Hz) is assigned to the strongly hydrogen-

(34) Graf, F.; Meyer, R.; Ernst, R. R. *J. Chem. Phys.* **1981**, *75*, 2914–2918.(35) Meier, B. H.; Graf, F.; Ernst, R. R. *J. Chem. Phys.* **1982**, *76*, 767–774.(36) Stoeckli, A.; Furrer, A. *Physica* **1986**, *136B*, 161–164.(37) Skinner, J. L.; Trommsdorff, H. P. *J. Chem. Phys.* **1988**, *89*, 897–907.(38) Horsewill, A. J.; Aibout, A. *J. Phys.: Condens. Matter* **1989**, *1*, 9609–9622.

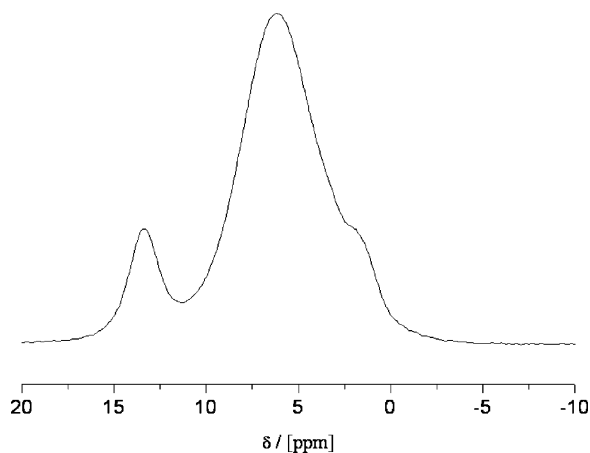


**Figure 5.**  $^1\text{H}$  MAS NMR spectrum of  $\alpha$ -truxillic acid measured at room temperature.

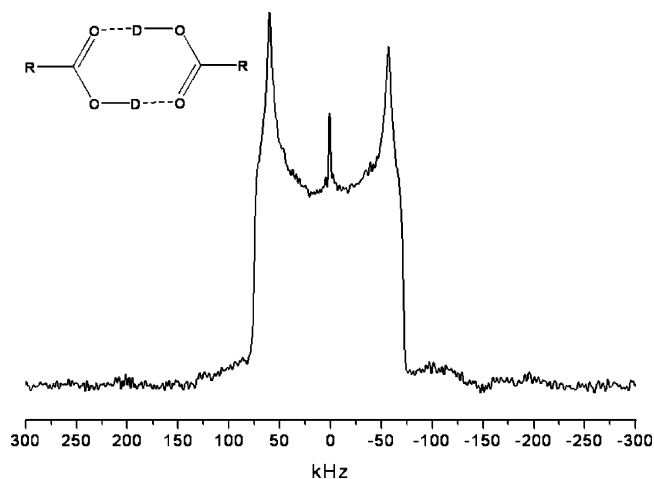


**Figure 6.** Solid-state  $^2\text{H}$  spectrum of  $\alpha$ -truxillic acid dimer at room temperature ( $\text{R} = (\text{C}_6\text{H}_5)_2, \text{C}_4\text{H}_4$ ). The quadrupolar splitting of NQCC = 155.9 kHz suggests a two site jump in the fast limit.

bonded carboxylic acid protons. In addition, variable-temperature NMR ( $T = 225 \text{ K}$  to  $T = 335 \text{ K}$ ) did not reveal any differences in the spectra indicating “constant” dynamics. Either to freeze-in possible motions very low temperatures (e.g., 30 K) would be necessary to clearly distinguish two different proton positions or the underlying motion of the proton is much faster than the NMR time scale yielding an averaged peak position. To unambiguously identify local mobilities, we focused on static, variable-temperature deuterium NMR measurements.

Larsen et al.<sup>39</sup> reported a perfect linear variation of the  $^2\text{H}$  nuclear quadrupolar coupling constant (NQCC) with the asymmetry of the hydrogen bond rendering NQCC a very useful parameter for determining the asymmetry of a given hydrogen bond. Generally the NQCC parameter for  $^2\text{H}$  increases with increasing asymmetry of the hydrogen bond, and for a long and asymmetric hydrogen bond it is about three times larger than that of  $^2\text{H}$  in a short symmetric hydrogen bond.<sup>40</sup> Thus, for asymmetric hydrogen bonds, the NQCC for  $^2\text{H}$  should be quite large.

The static  $^2\text{H}$  spectrum (cf. Figure 6) of an  $\alpha$ -truxillic acid dimer exhibits a Pake pattern with a quadrupolar splitting of

(39) Kalsbeek, N.; Schaumberg, K.; Larsen, S. *J. Mol. Struct.* **1993**, *299*, 155–170.

(40) Mayas, L.; Plato, M.; Winscom, J.; Mobius, K. *Mol. Phys.* **1978**, *36*, 753–764.

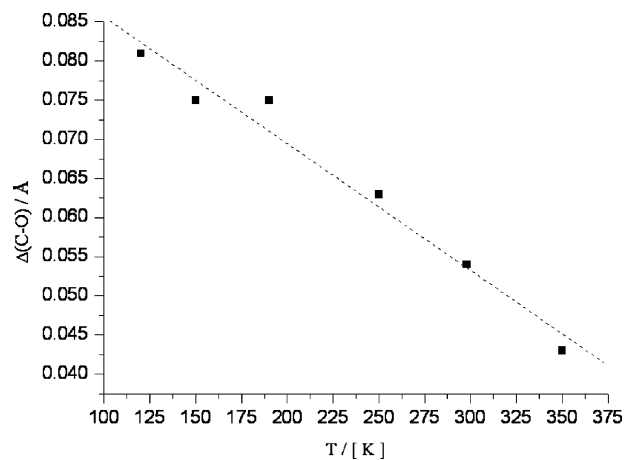


**Figure 7.** A plot of the  $\Delta(\text{C}-\text{O})$  values as a function of temperature showing that the truxillic acid C–O and C=O become less distinct with an increase of temperature. The plot shows an approximate linear fit. C–O and C=O distance variations vs temperature along with  $\Delta(\text{C}-\text{O})$  values are explicitly listed in the Supporting Information.

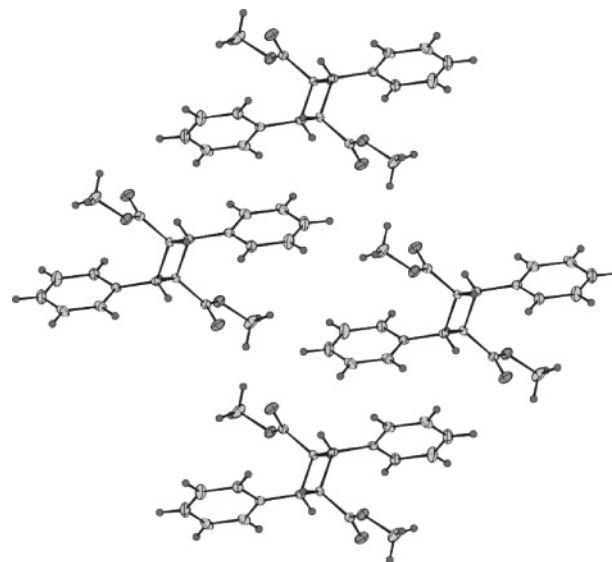


**Figure 8.** View of methyl ester of truxillic acid (dimethyl 2,4-diphenylcyclobutane-1,3-dicarboxylate) along  $b$ -axis.

NQCC = 155.9 kHz, which indicates the presence of certain dynamics, most probably reflecting a two site jump of a proton along the hydrogen bond in the fast limit. The sharp center peak is attributed to mobile deuterons that undergo pseudo-isotropic reorientations. The extracted NQCC parameter of 155.9 kHz is quite large and suggests the presence of long and asymmetric hydrogen bonds. This leads to the assumption that at a given time each truxillic acid molecule possesses two different carbonyl groups: one is an original carboxylic acid (COOH), and the other represents a carboxylate anion ( $\text{COO}^-$ ). In compounds that have asymmetric hydrogen bonds the two carboxy groups are different and give rise to different chemical shifts. The  $\delta$  ( $^{13}\text{C}$ ) is close to 180 ppm for carboxylate groups and close to 170 ppm for a carboxylic acid group.<sup>39</sup> The isotropic  $^{13}\text{C}$  chemical shift moved to higher frequencies as it passes from the carboxylic acid to the carboxylate form,<sup>23</sup> as noticed for truxillic acid as well, where the COOH signal appears at 178.9 ppm and the  $\text{COO}^-$  signal comes at a slightly higher frequency at 182.3 ppm. Hence, this results in a splitting of the cyclobutane ring signals. The intensities of the carbonyl signals are not equal,

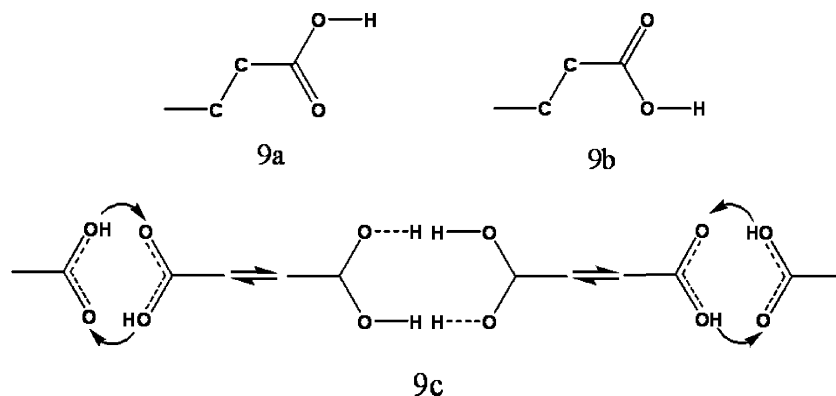


**Figure 9.** Conformations of a carboxyl moiety in a carboxylic acid: (a) synplanar conformation adopted by dimer; (b) antiplanar conformation adopted by monomer; (c) schematic representation of carboxyl moiety in the highest temperature (350 K) crystal structure of truxillic acid. Here, the proton is located in a double-well potential so that two half occupied positions for H are observed.

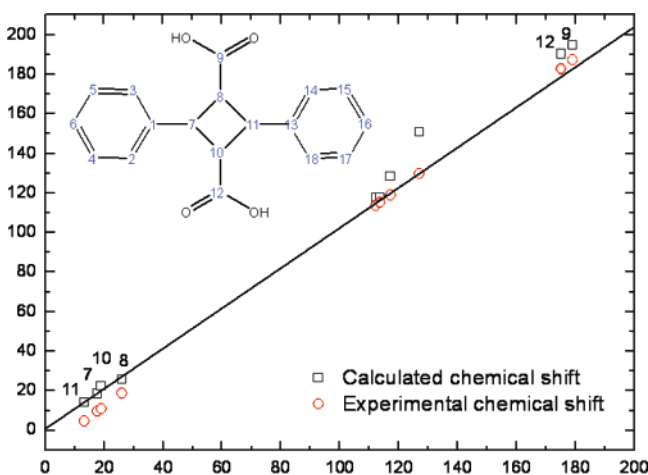


**Figure 10.** Plot of computed  $^{13}\text{C}$  chemical shifts for carboxylate anion of truxillic acid vs observed chemical shifts.

and this is more prominent at lower conversion; the carboxylate signal is less intense than its neighboring carboxylic acid signal, and it gradually increases as the conversion increases and becomes more or less equal to the carboxylic carbon signal after complete conversion. Dynamic hydrogen bonding also exists in the *trans*-cinnamic acid monomer as suggested by the high NQCC value of about 149.1 kHz, but this does *not* affect the  $^{13}\text{C}$ -CPMAS spectra (cf. Figure 2a); e.g., the carbonyl signals do not split. Most likely, this is due to the fact that  $\alpha$ -truxillic acid possesses two carbonyl groups on the same molecule while *trans*-cinnamic acid has one carbonyl atom. Since NMR measures an averaged chemical shift *no* splitting is observed in the case of the monomer.

The apparent discrepancy between NMR and X-ray analysis in the case of truxillic acid may result from two reasons: the carboxylic acid protons experience motion (dynamics) on the NMR time scale but appear rather rigid when observed by X-ray at very low temperature (30 K). Indeed, the presence of a carboxylate group in the compound is indicated by nearly equal C–O distances, with typical C–O values of 1.25–1.26 Å corresponding to a very small  $\Delta(\text{C–O})$  values.<sup>23,31,39</sup> The carboxylic acid group, COOH, with a C–O single bond ( $\approx 1.31$  Å) and a C=O double bond ( $\approx 1.21$  Å) has a  $\Delta(\text{C–O})$  value of around 0.1 Å. In the crystal structure of truxillic acid we observed that  $\Delta(\text{C–O})$  values are less than 0.1 Å, and a single C–O value is 1.312 Å, which is typical but the double bond is slightly larger than that in the carboxylic acid group (about 1.231

Å) yielding a  $\Delta(\text{C–O})$  less than 0.1 Å (0.081 Å). When we remeasured the crystal structure of the as-dimerized truxillic acid at different temperatures (120 K to 350 K), we observed a small gradual decrease of  $\Delta(\text{C–O})$  values at higher temperatures (cf. Figure 7). This trend is more prominent in the case of  $\alpha$ -*trans*-cinnamic acid monomer where  $\Delta(\text{C–O})$  is far less than 0.1 Å ( $\sim 0.038$  Å) pointing toward the presence of an asymmetric and a dynamic hydrogen bond in the carboxyl moiety of the monomer. We have also determined the crystal structure of truxillic acid methyl ester (the projection is given in Figure 8). The  $\Delta(\text{C–O})$  value amounts to 0.135 Å and clearly emphasizes an absence of carboxylates. This is quite expected since the ester cannot be involved in dynamic hydrogen bonding. Hence, the  $^{13}\text{C}$ -CPMAS NMR spectrum truly reflects centrosymmetry showing no peak splitting.

Leiserowitz has already discussed molecular packing modes of carboxylic acids.<sup>31</sup> He stated that in the crystal structures of  $\alpha$ ,  $\beta$ -saturated carboxylic acids  $\text{R–CH}_2\text{–CH}_2\text{–COOH}$ , the synplanar  $\text{C}^\beta\text{–C}^\alpha\text{–C=O}$  arrangement as shown in Figure 9a is adopted without *any* known exceptions, whereas the synplanar rule does not apply to the  $\alpha$ ,  $\beta$ -unsaturated acids  $\text{R–CH=CH–COOH}$ , with several compounds showing an antiplanar  $\text{C}^\beta\text{–C}^\alpha\text{–C=O}$  form. Concerning the photodimerization of  $\alpha$ -*trans*-cinnamic acid, the monomer (an  $\alpha$ ,  $\beta$ -unsaturated acid) adopts an antiplanar conformation while the resulting photodimer adopts a synplanar conformation.<sup>11,12</sup> Thus, upon increasing conversion ratios the molecule *slowly* changes from an antiplanar to a synplanar conformation, possibly facilitated by proton exchange since reactions in the solid state commonly occur with a minimum amount of atomic or molecular movement. This strongly supports the presence of dynamic disorder in the carboxyl moiety of truxillic acid where the proton undergoes rapid oscillations across the  $\text{O–H}\cdots\text{O}$  bond accompanied by interconversion between the carbonyl  $\text{C=O}$  and hydroxyl  $\text{C–O(H)}$  bond. The temperature dependence of  $\Delta(\text{C–O})$  in truxillic acid (cf. Figure 7) supports this assumption. Indeed, at the highest temperature (350 K) the search for the H-atoms by difference Fourier analysis revealed *two* carboxyl H atoms each occupied by 50%.

Finally, the  $^{13}\text{C}$ -CPMAS data were compared with *ab initio*  $^{13}\text{C}$  chemical shift computations of both  $\alpha$ -truxillic acid and its anion (created by arbitrarily removing one proton from the carboxyl group). Notably, the truxillic acid structure did not reveal any splitting, but the anionic structure yields a similar

signal splitting for the carbonyl and cyclobutane ring atoms as observed experimentally. Figure 10 shows the plot of computed  $^{13}\text{C}$  isotropic chemical shifts vs the observed values; the agreement is good in the range of  $\pm 5$  ppm.

#### 4. Conclusions

We have demonstrated that dynamic hydrogen bonding results in the appearance of additional signals in the  $^{13}\text{C}$  CPMAS spectra of photodimerized  $\alpha$ -*trans*-cinnamic acid. The transient asymmetry of the hydrogen bonds in the crystal temporarily destroys the photodimer's center of symmetry so that the truxillic acid molecules may exist in a noncentrosymmetric state in their crystal lattice. Indeed, this is a common phenomenon found for

a majority of carboxylic acid based dimeric compounds. Only the joint approach of both X-ray analysis and solid-state NMR successfully revealed the dynamic processes occurring in these topochemical reactions and, thus, provided detailed insight into the reaction mechanism of organic solid-state transformations.

**Supporting Information Available:** Powder diffraction data of both  $P2_1/n$  and  $C2/c$  phase, the  $^{13}\text{C}$  CPMAS spectrum of  $C2/c$  phase, a table of the C—O and C=O distance variations vs temperature along with  $\Delta(\text{C—O})$  values, full ref 30, and crystal structures provided as cif files. This material is available free of charge via the Internet at <http://pubs.acs.org>.

JA0773711